The Dependence of the Efficiency of Electrohydrodynamic Heat Exchanger on the Electric Conductivity of Liquid

Vladimir Chirkov, Ekaterina Rodikova, Yury Stishkov
St. Petersburg State University
phone: (7) 911-915-2698
e-mail: v.chirkov@spbu.ru

***Abstract*—Electrohydrodynamic flows are of great interest since they can be used to intensify heat exchange. However, the electric conductivity of liquid is usually disregarded and the model of unipolar injection is utilized. The paper studies the effect of liquid conductivity on the efficiency of EHD heat exchanger at the injection charge formation as well as at field-enhanced dissociation one. The investigation was carried out by means of the computer simulation of the complete set of EHD equations supplemented by heat transfer one. The estimation of the range of low-voltage conductivity of working liquid when electroconvection can be used for heat transfer enhancement was made.**

I. Introduction

Electrohydrodynamic (EHD) flows are of great interest, since they can be used to intensify heat exchange [1–6] and have a lot of advantages. Namely, EHD heat exchangers (EHDHE) feature very low power consumption, nearly unlimited operation life, the ability to operate in microgravity, and high efficiency at meso- and micro-scale as opposed to other approaches [7]. The above makes for the continuous increase in the number of research works on the topic; however, presently, there are actually no investigations, where the computer simulation and experiment are conducted concurrently, because the corresponding physics processes are highly complicated. Nevertheless, the development of numerical models of isothermal electroconvection lets bringing the simulation results nearer to quantitative level, and a number of investigations devoted to the comparison of experimental and numerical data were carried out [8–11]. In view of the above, the use of up-to-date simulation models for EHDHE computer-aided design is a topical issue and can provide quantitative evaluation of the device performance. To accomplish the latter, one has to allow for a number of factors that were separately touched upon as a subject in several papers: the effect of temperature on liquid properties [12], the dependence of the injection function on the electric field strength [11, 13], and the effect of

electrical conductivity of liquid on the injection EHDHE. The latter issue is one of the most topical and the paper is devoted to its investigation.

On the one hand, the effect of low-voltage conductivity (σ_0) on the intensity of EHD flow was studied as early as the previous century [14], and the maximum velocity was shown to decrease at $\sigma_0 > 10^{-8}$ S/m. On the other hand, the role of dissociation-recombination processes in the bulk are ignored whereas actual liquids show finite (non-zero) conductivity level that has to affect the intensity and structure of the flow. Besides, one cannot help noting the mirror-like problem in the investigation of EHD conduction pumping when the emergence of the injection reverses the net flow direction. The issue is investigated by the group of Prof. Yagoobi [15]

Finally, there is a quite different aspect concerning the electric conductivity, namely, the field-enhanced dissociation or the so-called Wien effect [16]. Previously, the charge formation mechanism was ignored by most researchers who studied EHD flows and believed to be a purely theoretical phenomenon. Recently, however, the situation changed due to the immediate experimental proofs that intensive EHD flows emerge due to the Wien effect [10, 17]. Moreover, the flow structure is rather similar to that of the injection electroconvection [18]. Therefore, the research into the effect of liquid conductivity on EHDHE performance has two sides: 1) the influence of dissociation-recombination processes on the injection electrohydrodynamic flow and 2) the possibility to design EHDHE of a new type basing on the Wien effect.

II. Mathematical and Computer Models

The investigation was carried out by means of the computer simulation of the complete set of EHD equations [14, 19] supplemented with heat transfer one:

$$div(\boldsymbol{E}) = \rho/\varepsilon\varepsilon_0 \tag{1}$$

$$\boldsymbol{E} = -\nabla\varphi \tag{2}$$

$$\partial n_i/\partial t + div(\boldsymbol{j}_i) = W_0 F(p) - \alpha_r n_1 n_2 \tag{3}$$

$$\boldsymbol{j}_i = n_i b_i \boldsymbol{E} - D_i \nabla n_i + n_i \boldsymbol{u} \tag{4}$$

$$W_0 = \sigma_0^2/(e(|b_1|+|b_2|)\,\varepsilon\varepsilon_0) \tag{5}$$

$$\alpha_r = e(|b_1|+|b_2|)/(\varepsilon\varepsilon_0) \tag{6}$$

$$\rho = e\,(n_1 - n_2) \tag{7}$$

$$\gamma\,\partial\boldsymbol{u}/\partial t + \gamma\,(\boldsymbol{u},\nabla)\boldsymbol{u} = -\nabla P + \eta\Delta\boldsymbol{u} + \rho\boldsymbol{E} \tag{8}$$

$$div(\boldsymbol{u}) = 0 \tag{9}$$

$$\gamma C_p\,\partial T/\partial t + \mathrm{div}(-k\nabla T + \gamma C_p\,\boldsymbol{u}T) = 0 \tag{10}$$

$$F(p) = I_1(2p)/(p) \tag{11}$$

$$p = e^2/(k_B T)\,\sqrt{(E/(4\pi\varepsilon\varepsilon_0 e))}, \tag{12}$$

where $\boldsymbol{E}$ is the electric field strength, ρ is the space charge density, φ is the electric potential, n is the ion concentration, $\boldsymbol{j}$ is the density of ion flux, $\boldsymbol{u}$ is the fluid velocity, P is the pressure, T is the temperature, ε is the relative electric permittivity, γ is the mass density, η is the dynamic viscosity, b is the ion mobility, D is the diffusion coefficient, C_p is the specific heat at constant pressure, k is the thermal conductivity coefficient; W_0 is the dissociation intensity, α_r is the recombination coefficient, ε_0 is the electric constant, e is the elementary electric charge, k_B is the Boltzmann constant, t is the time; subscript i indicates the ion species; I_1 is the modified Bessel function of the first kind; $F(p)$ is the Onsager function [16]. Ions are assumed to be monovalent. The set of equations is written for isothermal (and incompressible) liquid dielectric though the actual fluid properties are temperature dependent. However, the corresponding issue is beyond the present study and the dependences are omitted to simplify the analysis. Some relevant information can be found in [12]. Besides, the model disregards the buoyancy force (since the EHDHE can operate even in the microgravity) and heat radiation (as it is a separate process).

Computations were performed using software package COMSOL Multiphysics based on the finite element method. A blade-plane electrode system was chosen for the simulation since it featured highly non-uniform electric field distribution, which in turn promoted emergence of both the injection and field-enhanced dissociation mechanisms of charge formation. The geometry of computer model and boundary conditions for the set of equations are presented in Fig. 1. The lower plane represents both grounded electrode and heater simultaneously whereas the upper one is a cooler. The spatial size was chosen in such a way to be similar to that of typical microprocessor, i.e., several millimeters. The natural convection is much less efficient comparing to EHD on such a spatial scale due to high friction losses. The temperature drop between heater and cooler, ΔT, is 50° C, which corresponds to typical values of overheat for microprocessors. Besides, the results remain the same in the considered model if the overheat changes since liquid properties are independent of temperature. The voltage across the gap is reasonably set as great as possible but below the limit of cell breakdown strength since the efficiency of heat removal increases with the voltage. Here, it is 25 kV.

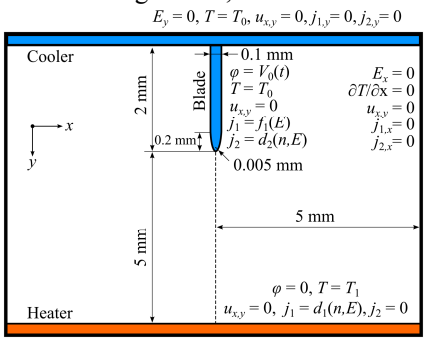

Fig. 1. Geometry of computer model and boundary conditions for the set of equations.

The choice of the injection function is a separate issue that is very complicated and under active consideration at the present time [11, 13, 20]. However, since the question

is still open, the linear function is used here with coefficients chosen to ensure the agreement in the order of magnitude between the total simulated current and realistic values for a cell with similar geometry [11]:

$$f_1(E) = A_1 (E - E_{st}) \cdot \vartheta(E - E_{st}), \tag{13}$$

where A_1 is the factor allowing for the intensity of the surface charge formation ($A_1 = 4 \cdot 10^9$ 1/(m^2·s)), E_{st} is the suggested threshold value of the injection onset ($E_{st} = 5 \cdot 10^6$ V/m), $\vartheta(E)$ is the Heaviside step function. It is believed that the charge loss is equal to the total current density for ions arriving to the boundary from the bulk:

$$d_i(n,E) = n_i b_i E_N - D_i \nabla_N n_i, \tag{14}$$

where subscript N denotes the normal to the surface of the electrode. In the first part of the next section, the injection charge formation at the blade surface and the charge loss at both electrodes are set, whereas the Wien effect is disregarded. The latter is included into consideration instead of the injection in the second part of the results.

The liquid properties correspond to those of transformer oil: $\varepsilon = 2.2$, $\gamma = 870$ kg/m^3, $\eta = 0.025$ Pa s, $|b| = 10^{-8}$ m^2/(V s) (which is assumed to be the same for ions of both polarities), $D = 1 \cdot 10^{-9}$ m^2/s, $k = 0.18$ W/(m K), $C_p = 2000$ J/(kg K). Low-voltage conductivity σ_0 is a parameter of study, and its value is varied (with other properties of the liquid left unchanged) in the range from 10^{-12} to 10^{-7} S/m.

The finite-element grid is constructed with allowance for features of unknown quantity distributions and has a mapped structure in the most important area (near both electrodes and within the central jet). The linear dimension of a finite element is about 1 μm near the blade tip and 5 μm near the heater surface. All computations are performed until the steady-state regime is attained and then the equality of inward and outward thermal fluxes is verified.

III. Results and Discussion

A. Injection EHDHE

EHD flow structure in the blade-plane electrode system is studied well enough in the case of the unipolar injection into initially non-conducting liquid (i.e., when $\sigma_0 = 0$ S/m). Ions emerge only at the blade tip and propagate to the counter electrode, which leads to the onset of an intensive electroconvection. The EHD jet strikes at the center of the plane electrode and spreads across its surface. If the latter is hotter than the liquid, the heat exchange takes place and the flow enhances thermal flux to the cooler. Introducing a small conductivity into the model fails to change the described distributions when the concentration of injected ions is many times that of ions emerged due to the dissociation. The corresponding results (for $\sigma_0 = 10^{-11}$ S/m) are demonstrated in Fig. 2 where distributions of space charge density, temperature contours, velocity and flow streamlines are presented. Fig. 2a shows the space charge to propagate through the interelectrode gap without considerable decrease in its magnitude; thus, the Coulomb force acts on the fluid within the whole gap providing high intensity of EHD flow.

As a result, the heat transfer within the bulk is provided mostly by electroconvection,

with isotherm 0.6 ΔT (Fig. 2a) nearly following a fluid streamline (Fig. 2b). The average heat flux density in the presented case is approximately 8 times the value that would be provided by the natural convection (at coefficient of thermal expansion $\beta = 6.5 \cdot 10^{-4}$ 1/K) in the same geometry (3.3 vs. 0.42 W/m^2).

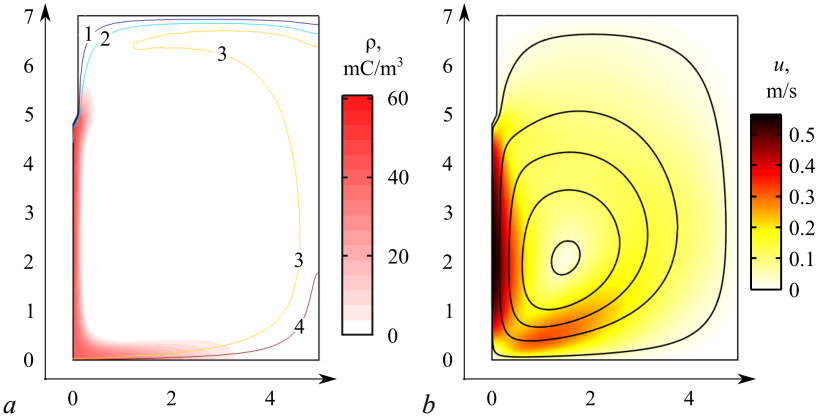

Fig. 2. (a) Surface plot of space charge density distribution and contour plot of relative temperature (1—0.2, 2—0.4, 3—0.6, and 4—0.8 ΔT), and (b) surface plot of fluid velocity and flow streamlines in an injection EHDHE at $\sigma_0 = 10^{-11}$ S/m.

The increase in liquid conductivity leads to the enhancement of the injected-ion recombination during ion motion toward the counter electrode. The main dimensionless parameter that evaluates the role of dissociation-recombination processes in the bulk (or the role of conductivity) is the ratio of two specific time scales—that of ion motion ($\tau_1 = L/u_a$, where u_a is the average fluid velocity) and charge relaxation time ($\tau_2 = \varepsilon\varepsilon_0/\sigma_0$). The mode change (i.e., $\tau_1/\tau_2 \approx 1$) is observed for typical electroconvection velocity during the increase in conductivity from 10^{-10} to 10^{-8} S/m. Besides, the conduction current density provided by negative ions begins to prevail over that of the injected positive ions near the blade surface in the conductivity range, which leads to the reversal of the polarity of near-electrode layer and the EHD flow direction.

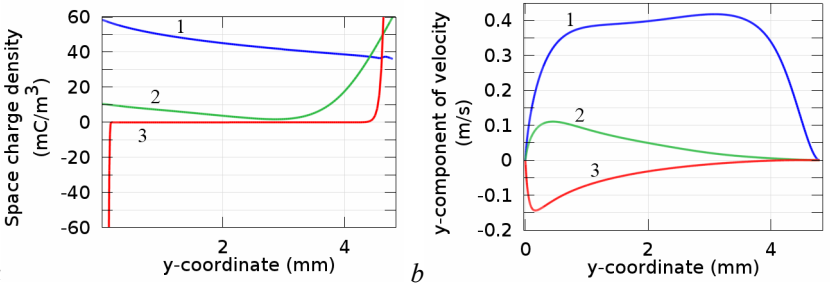

Fig. 3. Axial distributions of space charge density (*a*) and y-component of fluid velocity (*b*) in the injection EHDHE for three values of the conductivity (1—10^{-10}, 2—10^{-9}, and 3—10^{-8} S/m).

Fig. 3 presents axial distributions of space-charge and y-component of fluid velocity for three values of the conductivity (10^{-10}, 10^{-9}, and 10^{-8} S/m). The injection current

prevails over the conduction one and the EHD flow is directed toward the counter electrode in the first two cases (curves 1 and 2 in Fig. 3). However, the space charge recombines during its motion in the interelectrode gap in the second case causing the flow velocity to lessen by an order of magnitude. The flow direction is reversed in the third case when heterocharge emerges near both electrodes (curves 3 in Fig. 3a and b). All this leads to a considerable decrease in the average heat flux density from the hot plane with the increase in conductivity of working liquid (curve 1 in Fig. 4); however, the heat removal decreases down to non-zero value owing to the electroconvection-mode change from the ion-drag pumping to the conduction one. Some deviations of the approximation curve from the computed values are explained by the emergence of extra vortices in the bulk.

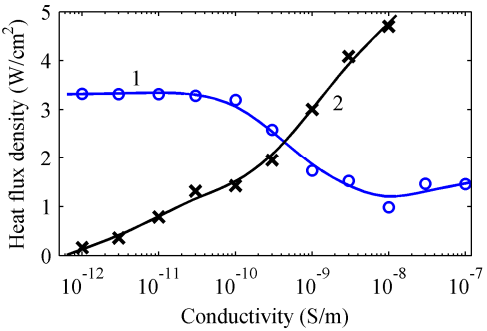

Fig. 4. The dependence of the average heat flux density on the liquid conductivity for two charge formation models: 1—injection and 2—field-enhanced dissociation; markers ("o" and "x") correspond to the computed values whereas curves are their approximation.

B. EHDHE Based on the Wien Effect

Reference [10] proves experimentally the Wien effect to lead to the emergence of intensive EHD flows; therefore, the charge-formation mechanism can underlie the EHDHE. Despite a relative increase in the dissociation rate under the effect of the strong electric field, which is independent of the low-voltage conductivity, the space charge emerging in the bulk appears to be proportional to its value. Thus, the intensity of EHD flows and efficiency of EHDHE based on the field-enhanced dissociation rise with the conductivity.

The fluid-velocity distribution and electroconvection streamlines are exemplified in Fig. 5a. The flow structure is seen to be very similar to that observed in the injection heat exchanger. However, the axial velocity distributions (Fig. 5b) show the EHD-flow intensity to rapidly increase with the conductivity. All this causes considerable enhancement in heat transport (curve 2 in Fig. 4), with the fluid velocity being even higher than that in the injection EHDHE. Thus, the electroconvection emerging owing to the field-enhanced dissociation is believed to be a very promising phenomenon to be utilized in heat exchangers.

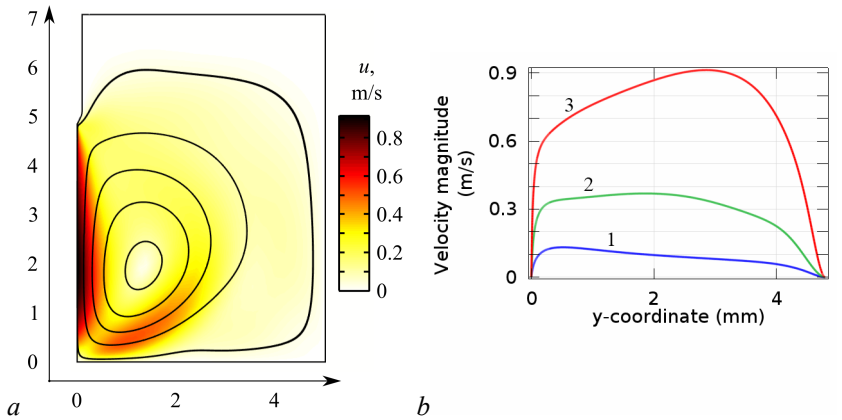

Fig. 5. Contour plot of fluid velocity and flow streamlines at $\sigma_0 = 10^{-9}$ S/m (a) and axial velocity distributions for three values of the conductivity (1—10^{-10}, 2—$3 \cdot 10^{-10}$, and 3—10^{-9} S/m) in an EHDHE based on the Wien effect.

IV. Conclusion

The increase in conductivity of working liquid leads to a steep decrease in the efficiency of the injection EHD heat exchanger due to the lessening of the flow intensity. However, efficient heat removal can be provided even in the case of heightened liquid conductivity if EHD heat exchanger bases on the field-enhanced dissociation mechanism of charge formation rather than the injection one.

Acknowledgment

The reported study was supported by RFBR, research project No. 15-08-07628. Research was carried out using resources provided by the Computer Center of SPbU and Center for Diagnostics of Functional Materials for Medicine, Pharmacology and Nanoelectronics of Research park of St. Petersburg State University.

References

[1] B. R. Lazarenko, F. P. Grosu, and M. K. Bologa, "Convective heat-transfer enhancement by electric fields," *Int. J. Heat Mass Transf.*, vol. 18, no. 12, pp. 1433–1441, 1975.

[2] M. K. Bologa, F. P. Grosu, and I. A. Kozhukhar', *Electroconvection and Heat Transfer*, Chisinau: Shtiintsa, 1977 (in Russian).

[3] P. Atten, F. M. J. McCluskey, and A. T. Perez, "Electroconvection and its Effect on Heat Transfer," *IEEE Trans. Electr. Insul.*, vol. 23, no. 4, pp. 659–667, 1988.

[4] F. M. J. McCluskey, P. Atten, and A. T. Perez, "Heat transfer enhancement by electroconvection resulting from an injected space charge between parallel plates," *Int. J. Heat Mass Transf.*, vol. 34, no. 9, pp. 2237–2250, 1991.

[5] V. K. Patel, F. Robinson, J. Seyed-Yagoobi, and J. Didion, "Terrestrial and microgravity experimental study of microscale heat-transport device driven by electrohydrodynamic conduction pumping," *IEEE Trans. Ind. Appl.*, vol. 49, no. 6, pp. 2397–2401, 2013.

[6] P. Traoré, A. Perez, D. Koulova, and H. Romat, "Numerical modelling of finite-amplitude electro-thermo-convection in a dielectric liquid layer subjected to both unipolar injection and temperature gradient," *J. Fluid Mech.*, vol. 658, pp. 279–293, 2010.

[7] M. R. Pearson and J. Seyed-Yagoobi, "Experimental study of EHD conduction pumping at the meso- and micro-scale," *J. Electrostat.*, vol. 69, no. 6, pp. 479–485, 2011.
[8] P. Traoré, M. Daaboul, and C. Louste, "Numerical simulation and PIV experimental analysis of electrohydrodynamic plumes induced by a blade electrode," *J. Phys. D. Appl. Phys.*, vol. 43, pp. 1–8, 2010.
[9] L. Yang, K. S. Minchev, M. Talmor, C. Jiang, B. C. Shaw, and J. Seyed-Yagoobi, "Flow distribution control in meso scale via electrohydrodynamic conduction pumping," in 2015 IEEE Industry Applications Society Annual Meeting, 2015, pp. 1–8.
[10] V. A. Chirkov, D. K. Komarov, Y. K. Stishkov, and S. A. Vasilkov, "Comparative analysis of numerical simulation and PIV experimental results for a flow caused by field-enhanced dissociation," *J. Phys. Conf. Ser.*, vol. 646, p. 012033, 2015.
[11] A. V. Gazaryan, A. A. Sitnikov, V. A. Chirkov, Yu. K. Stishkov, "A Method for Estimation of Functional Dependence of Injection Charge Formation on Electric Field Strength," in 2016 Electrostatics Joint Conference, 2016.
[12] J. Wu and P. Traoré, "A Finite-Volume Method for Electro-Thermoconvective Phenomena in a Plane Layer of Dielectric Liquid," *Numer. Heat Transf. Part A Appl.*, vol. 68, no. 5, pp. 471–500, 2015.
[13] J. Wu, P. Traore, C. Louste, L. Dascalescu, F. Tian, and A. T. Perez, "Numerical Investigation of Electrohydrodynamic Plumes for Locally Enhanced Cooling in Dielectric Liquids," *IEEE Trans. Ind. Appl.*, vol. 51, no. 1, pp. 669–678, Jan. 2015.
[14] Yu. K. Stishkov and A. A. Ostapenko, *Electrohydrodynamical Flows in Liquid Dielectrics,* Publishing House of Leningrad State Univ., Leningrad, 1989 (in Russian).
[15] M. Yazdani and J. S. Yagoobi, "The effect of uni/bipolar charge injection on EHD conduction pumping," *J. Electrostat.*, vol. 75, pp. 43–48, Jun. 2015.
[16] L. Onsager, "Deviations from Ohm's law in weak electrolytes," *J. Chem. Phys.*, vol. 2, pp. 599–615, 1934.
[17] J. C. Ryu, H. J. Park, J. K. Park, and K. H. Kang, "New electrohydrodynamic flow caused by the onsager effect," *Phys. Rev. Lett.*, vol. 104, no. 10, pp. 1–4, 2010.
[18] V. A. Chirkov, "Influence of charge formation mechanism on the structure of electrohydrodynamic flow in highly non-uniform electric field," *Saint Petersburg State University Studies in Physics*, vol. 1, 2013.
[19] A. Castellanos, *Electrohydrodynamics*, Wien: Springer, 1998.
[20] Y. K. Suh, "Modeling and simulation of ion transport in dielectric liquids - Fundamentals and review," *IEEE Trans. Dielectr. Electr. Insul.*, vol. 19, no. 3, pp. 831–848, 2012.